



Green mobility infrastructure: A techno-economic analysis of hybrid wind–solar PV charging stations for electric vehicles in Germany

Rahil Dejkam ^a , Reinhard Madlener ^{a,b,*}

^a Institute for Future Energy Consumer Needs and Behavior (FCN), School of Business and Economics / E.ON Energy Research Center, RWTH Aachen University, Mathieustraße 10, 52074 Aachen, Germany

^b Department of Industrial Economics and Technology Management, Norwegian University of Science and Technology (NTNU), 7491 Trondheim, Norway

ARTICLE INFO

Handling editor: X Ou

Keywords:

Electric vehicle
Stand-alone hybrid charging station
Hybrid renewable energy
Green mobility
Techno-economic feasibility

ABSTRACT

In the context of Germany's national energy transition and growing electric vehicle (EV) adoption, the development of cost-effective, region-specific EV charging infrastructure powered by renewable energy is crucial for achieving decarbonization targets. This study conducts a techno-economic assessment of stand-alone, battery-buffered electric vehicle charging stations (EVCSs) powered by hybrid solar photovoltaic (PV) and wind turbine (WT) energy systems in four major German cities: Berlin, Cologne, Hamburg, and Munich. Using the HOMER PRO simulation and optimization platform, the study identifies optimal system configurations that meet daily EV charging demand under location-specific meteorological conditions. Key economic indicators—Net Present Cost (NPC) and Levelized Cost of Electricity (LCOE) are evaluated to determine cost-effective solutions. Results indicate that hybrid PV/WT/battery systems are optimal for Berlin, Hamburg, and Munich, as they are able to NPC and LCOE while meeting daily charging demand and environmental targets. In Cologne, in contrast, due to higher wind availability, WT/battery systems emerge as the most cost-effective option. A sensitivity analysis quantifies the impact of varying load demand, storage capacity, solar irradiance, and wind speed on system performance, with NPC values ranging from €524,836 to €1,640,000 across various load scenarios. The findings demonstrate that economic feasibility can be further enhanced through PV tracking systems, increased wind turbine hub heights, and offshore wind deployment. The study provides actionable insights for designing regionally tailored, renewables-powered EV charging infrastructure in support of Germany's energy transition.

1. Introduction

Electric vehicles (EVs) have gained significant attraction in recent years as a means to reduce air pollution and greenhouse gas (GHG) emissions. However, the growing demand for EV charging infrastructure presents major challenges for long-term sustainability and scalability. Rising fuel prices, environmental concerns, and climate change have prompted governments worldwide, including the European Union (EU), to implement stringent regulations on fleet-level GHG emissions. In response, automakers are increasingly incentivized to develop low-emission, eco-friendly transportation solutions [1,2]. Among these, EVs have emerged as a promising alternative by reducing dependence on fossil fuels [3]. This paradigm shift has contributed to the declining cost competitiveness of internal combustion engine vehicles (ICEVs), especially as countries such as the United States (US), United Kingdom (UK),

China, and EU member states adopt policy measures such as financial subsidies, tax exemptions, and publicly funded infrastructure investments to accelerate EV deployment [4]. Many national strategies also aim to ensure that by 2050, EV fleets are powered entirely by renewable energy sources, thereby aligning with global decarbonization goals.

The increasing adoption of EVs has been further supported by the advancements in battery technologies and the growing availability of renewable energy-powered EV charging stations [5]. Nevertheless, consumer concerns—such as range anxiety, high purchase costs, battery safety issues, and inadequate charging infrastructure—remain significant market barriers, especially for long-distance travel where fast-charging capabilities are critical [6]. In response to these issues, governments worldwide are intensifying their efforts to develop sustainable EV ecosystems [3,7]. The energy savings, environmental

* Corresponding author. Institute for Future Energy Consumer Needs and Behavior (FCN), School of Business and Economics / E.ON Energy Research Center, RWTH Aachen University, Mathieustraße 10, 52074 Aachen, Germany.

E-mail address: RMadlener@eonerc.rwth-aachen.de (R. Madlener).

benefits of EVs, and strong policy support are expected to make them the dominant vehicle type in the automotive industry in the future [8]. In Germany, key policy frameworks such as the National Platform Electromobility (NPE), launched in 2010, and the National Electromobility Development Plan target the deployment of one million public charging stations nationwide by 2030 [9]. While various policy measures such as subsidies, tax incentives, and investments in charging infrastructure have been implemented, meeting these targets remains a significant challenge. The rising electricity demand caused by the rapid market diffusion of EVs is increasing the pressure on the electric grids. As EV charging demand is directly linked to power generation capacity and grid stability, ensuring a resilient and sustainable energy supply is crucial for the long-term success of e-mobility. One promising solution is the integration of renewable energy sources (RES) —particularly wind power and solar photovoltaics (PV) —into the EV charging infrastructure. Hybrid renewable energy systems (HRES) that combine RES with battery storage can reduce reliance on fossil-fuel-based power generation, lower emissions, and enhance energy security [10]. In Germany and across Europe, solar and wind energy are expected to play a pivotal role in achieving climate neutrality [11]. However, the techno-economic feasibility of such renewables-powered (EVCSs) is highly dependent on local renewable resource availability, which varies significantly across different geographic locations. This variability presents a core challenge in designing optimal system configurations. In recent years, Al-Quraan et al. [12–19] have proposed a comprehensive series of studies applying techno-economic predictive control, bi-/tri-level optimization, and sizing techniques for stand-alone and grid-connected HRES. These works explore multi-layer control architectures and advanced forecasting methods to enhance the performance of HRES under uncertain demand and renewable supply conditions. Their contributions demonstrate how predictive control and layered optimization frameworks can significantly improve system efficiency and cost-effectiveness across diverse application scenarios.

Despite the methodological sophistication of these studies, they do not address EV charging infrastructure, nor do they consider location-specific renewable energy availability—both of which are essential for real-world, urban deployment scenarios. Moreover, most studies focus on generalized HRES or microgrid applications without tailoring the analysis to stand-alone configurations for EV charging under mobility-driven demand profiles.

To address this research gap, the present study proposes a techno-economic simulation framework to evaluate the optimal configuration and operational feasibility of stand-alone hybrid EVCSs powered by PV, WT, and battery storage. Focusing on four major German cities, the model uses Hybrid Optimization of Multiple Energy Renewables (HOMER) PRO to simulate system performance under location-specific solar and wind resource conditions and EV demand profiles. The findings provide actionable insights to inform regional infrastructure planning and contribute to Germany's broader goal of achieving a carbon-neutral transport sector.

2. Literature review

Several studies have evaluated the techno-economic feasibility of grid-connected and stand-alone hybrid EV charging systems, employing a variety of modeling techniques. Tools such as HOMER PRO have been widely adopted to assess optimal system configurations, cost-effectiveness, and environmental performance under different climate and operational conditions.

A notable contribution by Al Wahedi and Bicer [20] investigated the techno-economic feasibility of a stand-alone PV/battery EVCS under desert conditions in Qatar, demonstrating that location-specific optimization significantly enhances system viability in harsh climate environments. Li et al. [21] extended this approach in China by comparing hybrid PV/WT/battery configurations across several Chinese cities. Their study showed that PV/WT/battery systems can be cost-effective,

but their economic viability is highly dependent on regional climatic conditions. Among the cities analyzed, Nanjing emerged as the most economically feasible location, while Zhengzhou was found to be the least feasible.

In Brazil, Schetinger et al. [10] simulated the integration of a PV-powered EV charging system on a university campus and concluded that integrating EVs with clean energy can significantly reduce emissions while maintaining cost efficiency. Similarly, Ekren et al. [22] optimized a hybrid PV/WT EVCS in Izmir, Turkey, revealing a feasible configuration with a generating capacity of 843,150 kWh/a and a production cost of 0.064 €/kWh, though they did not evaluate which variables influence cost performance most. While these studies underscore the advantages of renewables-powered EVCSs, they also highlight that the optimal system configuration and cost-effectiveness depend heavily on location-specific factors.

In addition to location-specific optimization, energy storage has emerged as a central theme in assessing stand-alone EVCSs. Grande et al. [25] investigated the techno-economic feasibility of a stand-alone PV/battery hybrid system for charging EVs in Madrid, Spain, finding that battery storage capacity significantly impacts cost-effectiveness, especially in regions with seasonal solar variability. For the Netherlands, Mouli et al. [26] examined workplace PV/battery chargers and found that battery size must be tailored to local irradiance patterns to reduce grid dependence. Karmaker et al. [23] suggested a hybrid solar PV/biogas-powered EVCS to reduce the load on the national grid. Using the HOMER software, they evaluated the technical, economic, and environmental sustainability of the proposed system. The optimal design, with a total NPC of 56,202 €/kWh, an operational cost of 2540 €/a, and a LCOE of 0.1302 €/kWh, was found to have the lowest overall costs. The proposed solution reduced CO₂ emissions by 34.7 % compared to standard grid-based charging stations. In another study, Karmaker et al. [24] conducted a thorough feasibility study of the planned EVCS using the HOMER model, considering technical, economic, and environmental aspects. They created a 20 kW charging station for electric vehicles using biogas resources in Bangladesh. According to the findings, this station can provide the daily charging needs of 15–20 EVs, including simple bicycles and electric three-wheel EVs. By using this station instead of grid charging, users can save between €16.3 and €29.5 per month per vehicle, highlighting its economic benefit.

The overall system configuration and operational strategy play a crucial role in determining the feasibility of renewable energy-powered EV charging infrastructure. Vermaak and Kusakana [27] examined the feasibility of installing EVCSs powered by renewable energy in the rural Democratic Republic of the Congo. Their study applied the least beneficial month sizing method to configure the capacity of system components such that the PV and wind energy sources, ensuring that they could meet demand even in months with lower renewable energy availability. Two different charging station operation strategies were simulated, and the results examined to ascertain the optimal system configuration. The simulation results demonstrate that using the charging station continually to charge several vehicles throughout the day or 24 h was the optimal operation strategy. Similarly, Alghoul et al. [28] assessed the performance of a PV/grid hybrid charging system under various grid capacity scenarios. The outcomes show that a solar-aided EV charging system, integrated into a gasoline station and a 10 kW limited power grid, could meet the initial EV penetration rate of 2.14 %. With a feed-in-tariff plan, the capital cost of the 10 kW PV/microgrid system can be recovered in 6.3 years, providing 14.7 years of net profit based on an assumed 21-year system lifetime.

Recent studies have introduced advanced optimization and control frameworks to enhance hybrid EV charging infrastructure. Dong et al. [29] developed a two-stage stochastic scheduling model for integrated PV/battery EV charging systems that addresses uncertainties in photovoltaic (PV) generation and battery power constraints. Their approach improves system reliability by dynamically allocating energy resources under varying solar conditions and vehicle demand profiles. In a related

advancement, Tabassum et al. [30] proposed an adaptive energy management strategy for sustainable EVCSs within hybrid microgrid architectures. Their framework integrates real-time forecasting and load balancing to optimize energy flows from PV, WT, and battery systems, enhancing operational efficiency and grid independence. However, these contributions focus primarily on microgrid or semi-grid-connected scenarios and do not assess stand-alone system behavior or location-specific renewable energy potentials.

A summary of these key studies is provided in Table 1, which outlines their geographic scope, renewable energy types, modeling tools, and major contributions. This table helps contextualize the existing body of work and highlights where gaps remain.

The key contributions of the present study are:

Despite extensive advancements in renewable-powered EV infrastructure research, no existing study provides a comparative techno-economic evaluation of stand-alone hybrid PV/WT/battery EV charging systems across different cities in Europe (Germany). Prior research often focuses on PV-only systems or evaluates hybrid systems in isolated locations, overlooking the value of wind/solar integration despite Germany's high wind energy availability. Moreover, sensitivity analysis of key operational variables such as demand profiles, capacity shortages, solar irradiation, and wind speed is often limited or absent, leaving uncertainty about the robustness of system design choices under real-world conditions.

This study addresses these gaps by conducting a comparative techno-economic analysis of stand-alone PV/WT/battery EV charging systems in four major German cities with varying renewable energy source profiles: Berlin, Cologne, Hamburg, and Munich. By incorporating empirical meteorological data, realistic EV demand modeling, and scenario-based sensitivity analysis, the research delivers regionally tailored insights into infrastructure planning for renewables-based EV charging systems.

The remainder of the study is structured as follows. Section 2 describes the methodology of the study and presents the setup for the four case studies of hybrid EVCSs in the four cities in Germany considered. Section 3 presents the results and a discussion of these; finally, Section 4 concludes.

3. Methodology

3.1. Energy simulation tool

The HOMER PRO software developed by the US National Renewables Energy Laboratory (NREL) is the software tool applied for simulation and optimization in this study. HOMER employs grid search and proprietary derivative-free optimization techniques to determine the most economically viable solution. The methodology flowchart for this study is shown in Fig. 1, and each stage is explained in more detail in the following.

The methodology illustrated in Fig. 1 begins with the definition of input parameters—such as renewable energy sources availability, EV charging load profiles, component specifications (e.g., PV, wind, battery, converter), technical constraints, and economic data. These inputs are fed into HOMER's simulation engine, which evaluates all feasible system configurations by minimizing the NPC under user-defined constraints. Infeasible configurations are discarded, and feasible ones are ranked based on economic performance. In the final phase, a multi-dimensional assessment is conducted, including techno-economic-environmental analysis and sensitivity testing (e.g., variation in load, wind speed, or storage capacity), to identify robust system designs under different operating conditions.

The economic optimization in this study is based on minimizing the net present cost (NPC), which reflects the total lifecycle cost of the system over 25 years, including capital, replacement, O&M, and fuel costs (where applicable). Although other indicators like LCOE are reported for interpretive purposes, NPC serves as the main cost function driving the optimization process in HOMER PRO.

3.2. Assessing the economic feasibility

The most famous indicators applied by renewable energy power generation systems are *NPC* and *LCOE*, followed by *PP*, *PI*, and *IRR*, all described next. The total *NPC* of the system is calculated as (see Refs. [20,31]):

$$NPC = \frac{C_{\text{total annual}}}{\frac{i(1+i)^T}{(1+i)^T - 1}} \quad (1)$$

where $C_{\text{total annual}}$ represents the total annualized cost, n denotes the economic operational lifetime in years, and t refers to a specific year ($t =$

Table 1
Summary of key studies on hybrid renewable-powered EV charging stations.

Study	Year	Country/Region	System Type	RES Type	Tool/Method	Key Contribution
Alghoul et al.	2018	Malaysia	Grid-connected	PV	HOMER	• Evaluated feed-in tariff profitability for grid/PV charging station
Al Wahedi & Bicer	2021	Qatar	Stand-alone	PV, Battery	HOMER	• Demonstrated feasibility of site-specific renewables-powered EV stations under desert conditions
Dong et al.	2024	China	Grid-connected	PV, Battery	Two-stage stochastic model	• Improved energy dispatch reliability under PV and load uncertainty for EV charging infrastructure
Ekren et al.	2022	Turkey	Stand-alone	PV, WT	HOMER	• Identified optimal configuration and energy cost for Izmir
Grande et al.	2021	Spain	Stand-alone	PV, Battery	HOMER	• Evaluated battery sizing impacts in seasonal climates
Karmaker et al.	2020	Bangladesh	Stand-alone	PV, Biogas	HOMER	• Achieved 34.7 % CO ₂ reduction vs grid-based charging
Karmaker et al.	2021	Bangladesh	Stand-alone	Biogas	HOMER	• Designed 20 kW station for light EVs; highlighted monthly user savings
Li et al.	2020	China	Stand-alone	PV, WT, Battery	HOMER	• Compared cost-effectiveness across Chinese cities; found regional variability significant
Mouli et al.	2016	The Netherlands	Grid-connected	PV, Battery	Simulation model	• Examined workplace charging feasibility under seasonal PV generation
Schetinger et al.	2020	Brazil	Grid-connected	PV	HOMER	• Showed GHG reductions on a university campus through integrated renewables-powered EV charging systems
Tabassum et al.	2025	India	Microgrid-based	PV, WT, Battery	Adaptive EMS (ANFIS-based)	• Developed real-time load balancing and control for hybrid EV stations with enhanced off-grid resilience
Vermaak & Kusakana	2014	DR Congo	Stand-alone	PV, WT	Least-beneficial month sizing	• Optimal operation strategy for rural Tuk-tuk stations

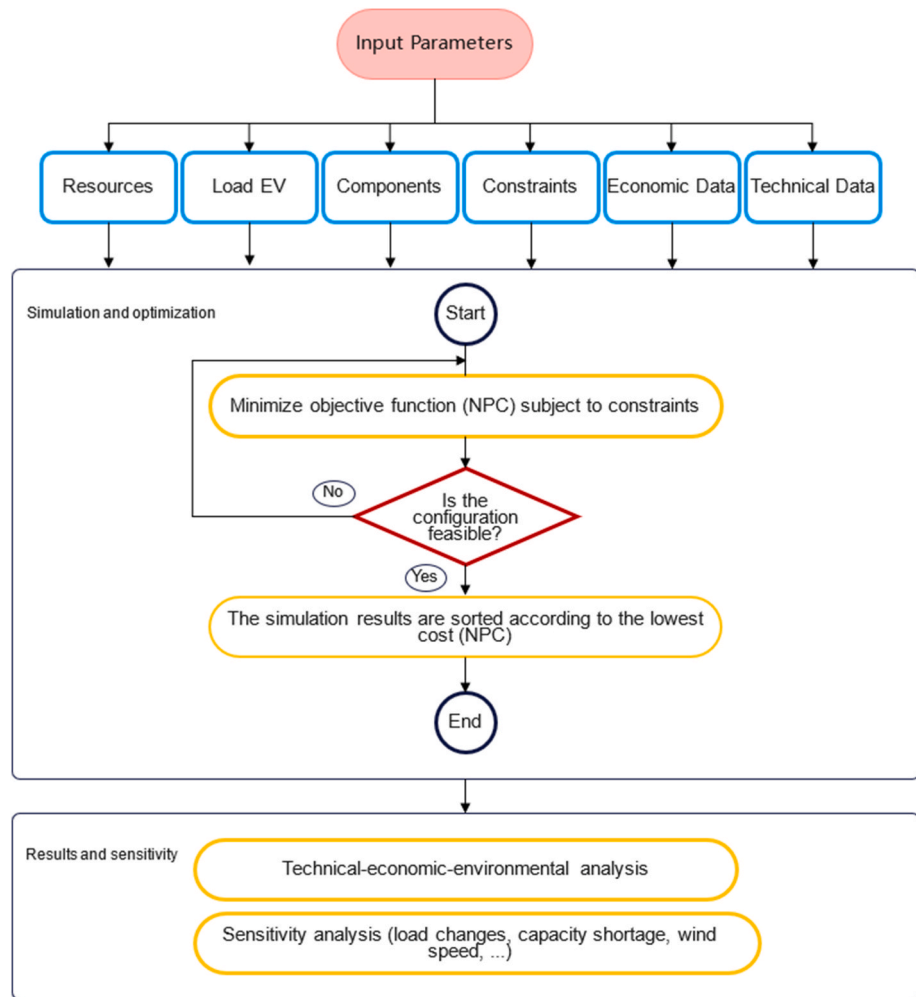


Fig. 1. Methodology flowchart.

1, 2, .., T). NPV is the present value of all investments and lifetime costs associated with constructing and operating an electricity generation plant, minus the present value of all revenues generated by the plant over its lifespan. $LCOE$ is the present value of the total costs of building and operating an electricity generation plant, divided by the total electricity generated over its lifetime. It represents the average cost per kWh required to supply electricity under a given proposal and is calculated as (see Refs. [20,32]):

$$LCOE = \frac{I_0 + \sum_{t=1}^T \frac{A_t}{(1+i)^t}}{\sum_{t=1}^T \frac{M_{el}}{(1+i)^t}} \quad (2)$$

where I_0 denotes the investment expenditure at $t = 0$, A_t is the annual total costs in year t , M_{el} is the electricity produced in the respective year t [kWh], i the discount rate, and T the expected economic operational lifetime in years.

To complete the economic analysis, additional economic assessment metrics such as payback period (PP), profitability index (PI), and the internal rate of Return (IRR) have been computed and compared for stand-alone and grid-connected systems.

The PP calculation measures how long it will take for cash inflows from an investment to equal the initial cash outflows over a given time period.

According to equation (3) below, the profitability index (PI) is determined by dividing the present value of future cash flows by the initial investment:

$$PI = \frac{\sum_{t=1}^T \frac{CF_t}{(1+r)^t}}{I_0} \quad (3)$$

where CF_t is the future cash flow (€) in each time period t , I_0 denotes the initial investment (€), r the discount rate (%), and T the number of time periods considered.

Finally, IRR is calculated using the following formula:

$$IRR = \sum_{t=1}^T \frac{CF_t}{(1+r)^t} - C_0 \quad (4)$$

where C_t is the net cash inflow during period t (€), C_0 the total initial investment (€), r the discount rate (%), and t the number of time periods considered.

3.3. Case study

Until 2014, Germany had the most extensive installed solar PV capacity in the world at about 1.9 GW; by 2021, that capacity has increased to over 58 GW. Germany ranks second for offshore wind, with over 7 GW, and third in terms of total installed wind generating capacity, at 64 GW in 2021 (compared to 59 GW in 2018). The label "the world's first big renewable energy economy" has been applied to Germany (see Ref. [33]).

In this paper, hybrid stand-alone EVCSs in the four major cities Berlin, Cologne, Hamburg and Munich are chosen as four case studies. These cities were chosen due to their geographical diversity, population density, and economic significance, which influence the feasibility and scalability of renewable energy-based EV charging infrastructure. Their locations in different climate zones allow for an in-depth analysis of regional variations in solar and wind energy potential, providing

insights into how geographical differences affect hybrid charging station performance. Additionally, these cities have the highest EV adoption rates in Germany, driven by strong transport policies, infrastructure investments, and urban mobility initiatives [34]. Studying these urban areas allows for an evaluation of how existing EV market penetration, grid integration challenges, and consumer behavior impact the feasibility of hybrid renewable charging systems. The geographical coordinates are shown in Table 2 and Fig. 2.

3.3.1. Load data

The load data in this study is modeled under hypothetical conditions to represent a small-scale EV charging scenario, assuming a fleet of 40 EVs operating within an urban setting, each with an average battery energy requirement of 30 kWh/d, leading to a total estimated daily energy demand of 1200 kWh. Based on the data either fed into the HOMER model manually or retrieved from the HOMER library, the software performs hourly simulations over a one-year period, evaluating all possible system configurations to identify the optimal setup that satisfies both demand and technical criteria at the minimum lifecycle cost [20].

The daily and seasonal stochastic EV load profiles are shown in Fig. 3, illustrating how the EVCS electricity demand is predicted in HOMER Pro. The daily profile reveals that charging demand steadily increases from early morning, and peaks between 12:00 and 18:00 h, aligning with workplace and public charging station usage trends. The seasonal profile indicates moderate variations in demand across months, suggesting that EV charging patterns remain relatively stable throughout the year. The yearly profile highlights a consistent hourly load distribution, with peak fluctuations occurring during midday and early evening. The estimated annual average daily energy demand is 1200 kWh, with an observed peak-load of approximately 200 kW. The black zones in the yearly profile indicate minimal or no charging activity between 0:00 and 6:00 h, confirming that most EV charging occurs during the daytime and early evening. The same load profile is applied to all selected cities due to the similar urban characteristics and EV adoption trends observed in large metropolitan areas. Previous studies have demonstrated that EV charging behavior in major cities is primarily influenced by commuting patterns, workplace and residential charging infrastructure, and electricity pricing policies rather than geographical location alone [36]. Given the lack of high-resolution, city-specific EV charging data, this generalized load profile provides a reasonable approximation for urban EVCS planning. While the load profile reflects typical hourly and seasonal charging behavior, it does not account for time-of-use pricing or dynamic user response to electricity tariffs, which are beyond the scope of this analysis. Furthermore, although the load profile remains constant, this study accounts for regional differences in renewable energy availability (solar and wind potential) to evaluate location-specific system performance.

3.3.2. Resource assessment

This study uses hybrid renewable energy resources for powering the EVCSs, including a PV/WT/battery hybrid system. Consequently, in this part, the assessment of meteorological data is provided.

3.3.3. Weather data

Monthly average wind speeds at 50 m/s above ground over 30 years (from January 1984 to December 2013) for each selected location are

Table 2

Geographical coordinates of the chosen sites.

City	Federal State	Latitude (°N)	Longitude (°E)	Average Solar Irradiation (kWh/m ² /day)	Average Wind Speed (m/s)	Population (2024)
Berlin	Berlin	52.5214	13.4050	2.73	6.64	3,897,145
Hamburg	Hamburg	53.5511	9.9937	2.72	7.07	1,861,053
Munich	Bavaria	48.1351	11.5820	3.15	4.82	1,594,632
Cologne	North Rhine-Westphalia	50.9375	6.9603	2.82	6.62	1,149,014



Fig. 2. Map of Germany with the four city case studies investigated [35].

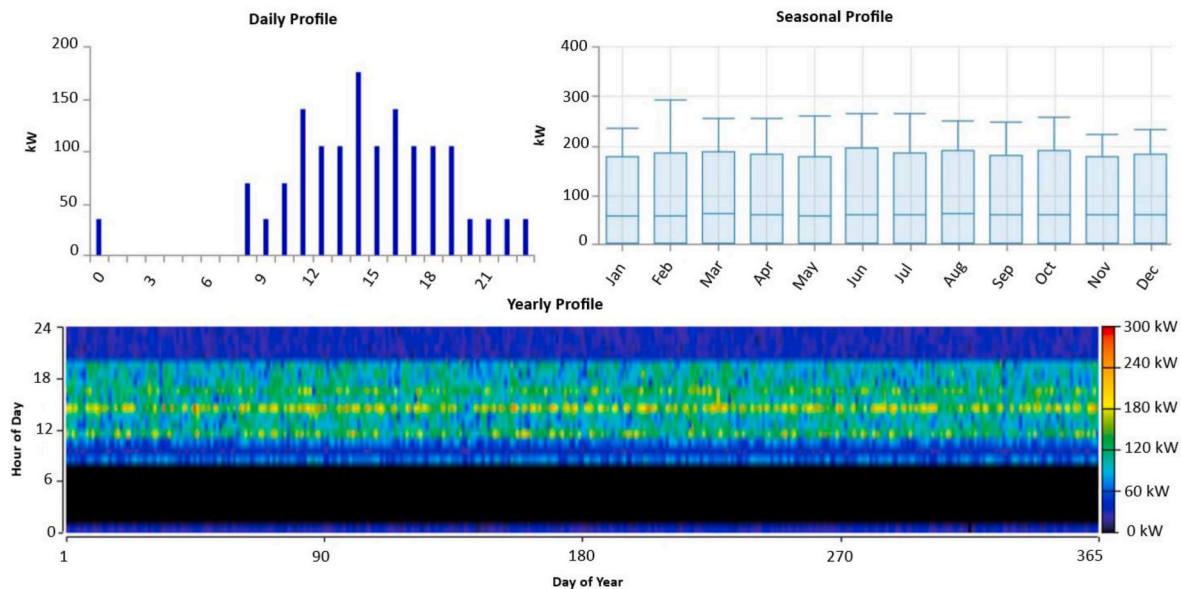


Fig. 3. Load profile for the charging stations in the four cities in Germany.

extracted from the National Aeronautics and Space Administration (NASA) forecasting of the Worldwide Energy Resource (POWER) database [37]. In Fig. 4, the monthly average wind speed data for 30 years

are illustrated. The maximum average wind speed values for Berlin, Hamburg, Munich and Cologne occur in January. The average wind speed values from 1984 to 2013 for Berlin, Hamburg, Munich and

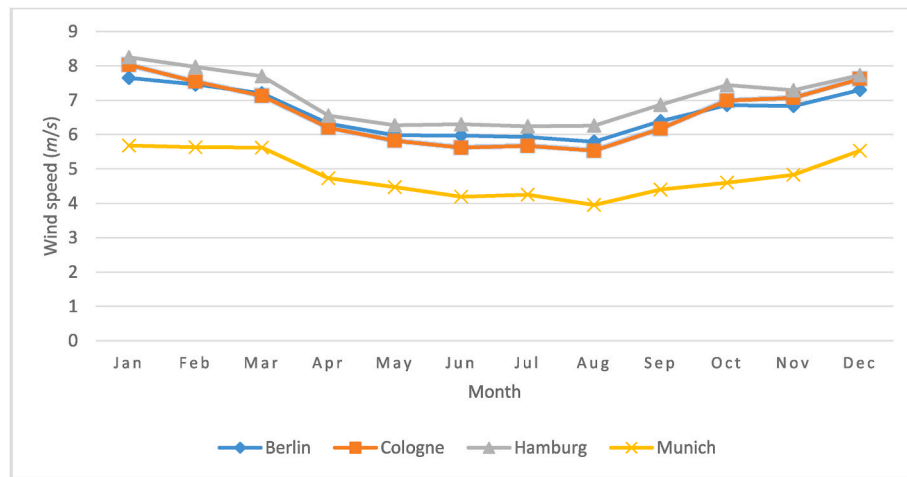


Fig. 4. Monthly average wind speed at the four chosen locations.

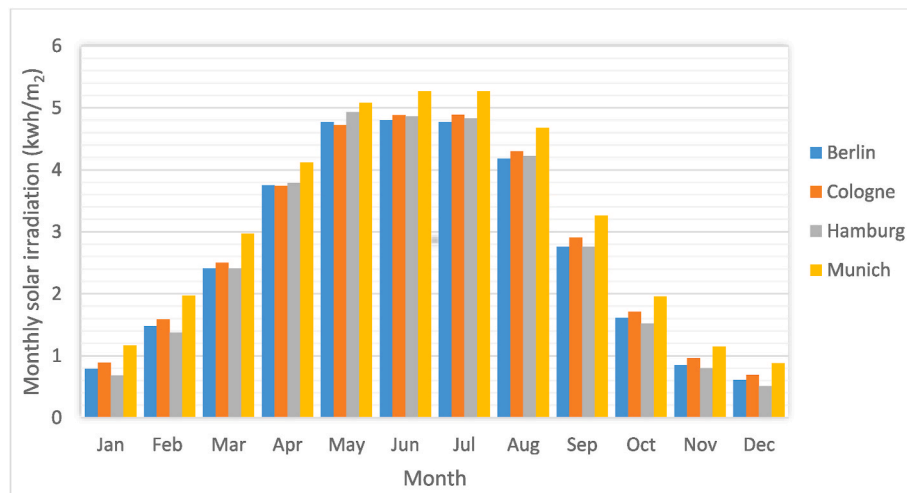


Fig. 5. Monthly average solar irradiation data at the four chosen locations, July 1983– June 2005.

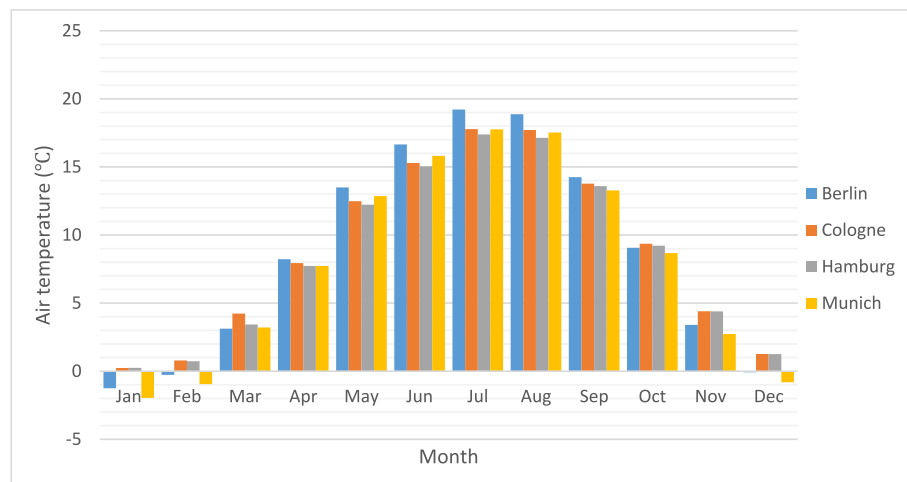


Fig. 6. Monthly average air temperature data for the four chosen locations, January 1984–December 2013.

Cologne were 6.64 m/s, 7.07 m/s, 4.82 m/s, and 6.62 m/s, respectively (Table 1; [33]). These high wind speeds during the winter months could potentially enhance wind energy production, particularly in Hamburg,

which shows the highest average wind speeds, closely followed by Berlin and Cologne (see Fig. 4).

Monthly average solar Global Horizontal Irradiance (GHI) data of the

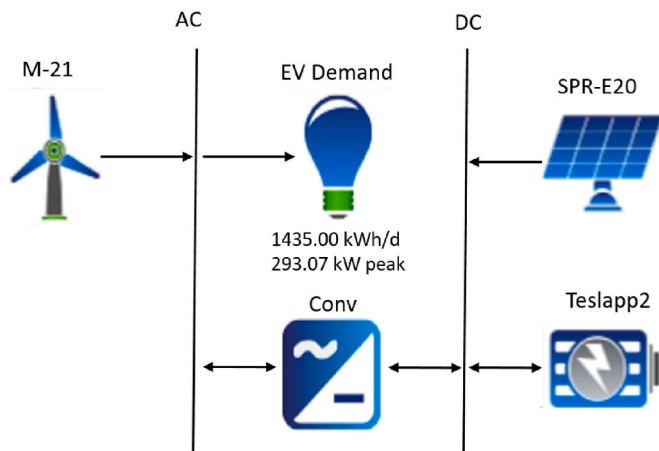


Fig. 7. Schematic of the hybrid EV charging system showing energy flows from PV, WT, and battery components to the load.

four specific cities over 22 years, from July 1983 to Jun 2005, were also taken from the NASA Prediction of Worldwide Energy Resource (power) database. Fig. 5 illustrates the monthly average GHI data for the four cities studied [37]. As can be seen, solar irradiation in the southern city of Munich is considerably higher than in the others. The variability in GHI data across different months highlights the need for solar energy systems that can adapt to lower light conditions during certain periods, especially considering the significant drop in solar irradiance during the winter months.

NASA's Prediction of the Worldwide Energy Resource database is used to acquire monthly average air temperature data for the four chosen locations for 30 years from January 1984 to December 2013 as an additional input parameter [37]. Fig. 6 shows the monthly average air temperature data in the four different cities studied. For Berlin, Hamburg, Munich and Cologne, January's minimum monthly average air temperature values were -1.25°C , 0.24°C , 0.25°C , and -1.96°C , respectively. On the other hand, the maximum monthly average air temperatures of 19.22°C , 17.76°C , 17.78°C , and 17.39°C were recorded in the month of July in Berlin, Hamburg, Munich, and Cologne, respectively. These temperature extremes highlight potential challenges in maintaining optimal operational conditions for both wind turbines and solar panels. Low air temperatures in winter can improve the efficiency of PV arrays, while high air temperatures in summer might negatively affect the performance of wind turbines.

3.4. System configuration and modeling

The project lifetime of the hybrid charging systems is set to 25 years. An inflation rate of 2 % and annual discount rate of 8 % are assumed, with calculations adjusted accordingly on an annual basis. According to Fig. 7, the off-grid hybrid PV/WT/battery EV charging system consists of PV arrays, WTs, batteries, converters, and other components. These are

Table 3
Specifications of the SunPower E20-327 PV solar panel.

Parameter	Specification	Unit
PV slope	30/32/35/30.6	°
Nominal operating cell temperature	45	°C
Temperature effects on power	-0.38	°C
Derating factor	88	%
Efficiency of PV arrays at STC	20.4	%
Capital cost	1300	€
Replacement cost	1100	€
O&M cost	20	€/a
Capacity (range)	0-3000	kW
Lifetime	25	a

Table 4

Parametrization of the XANT M – 21 (100 kW) wind turbine, manufactured by XANT.

Parameter	Specification	Unit
Rotor diameter	21	m
Hub height	31.8	m
Number of wind turbines (range)	0-20	-
Lifetime	20	a
Cut-in wind speed	3	m/s
Cut-out wind speed	20	m/s
Rated capacity	100	kW
Rated wind speed	11	m/s
Capital cost	50,000	€
O&M cost	2500	€/a
Replacement cost	30,000	€

integrated through a shared DC/AC bus, allowing the system to operate as a stand-alone microgrid capable of autonomous energy balancing without reliance on the utility grid.

Batteries serve as the primary energy storage technology (see section 2.4.3 below for details) used. WT and, to some extent, PV power generation provide the majority of the power for EVCSs. The extra power will be charged to the battery when the amount of power produced by the PV arrays and WTs exceeds the demand for charging. Instead, the load will be provided by the batteries (cf. [24,38]).

If the batteries are fully charged and renewable power generation continues to exceed load demand, excess energy is curtailed. This curtailment behavior is inherent in HOMER PRO's load-following dispatch logic and reflects a realistic operational constraint in off-grid systems without auxiliary loads. HOMER PRO dynamically manages power flow using a load-following dispatch strategy, prioritizing renewable energy sources and utilizing storage when necessary. The bidirectional converter enables smooth DC/AC transitions and ensures reliable power supply to EVCSs in the absence of a grid connection. This setup allows for real-time power routing in response to varying load conditions, as schematically represented in Fig. 7.

To support the techno-economic analysis, the system's technical behavior was modeled in detail. Component-level performance including PV power output under location-specific solar irradiation, wind turbine generation using height-adjusted wind speed and power curves, and battery charge-discharge cycles governed by round-trip efficiency and depth of discharge (DoD) was simulated using HOMER PRO. The control strategy follows a load-following dispatch logic, prioritizing renewable power generation for direct consumption and storing surplus energy in batteries. Full mathematical formulations and sensitivity parameters are provided in Appendix A.

3.4.1. PV module

One of the fundamental technologies used in the creation of Hybrid Renewable Energy Storage (HRES) systems is the PV module. The estimated capital, replacement, and maintenance costs of a solar PV module are 1300 €/kW, 1100 €/kW, and 20 €/a, respectively [39–41]. Detailed equations and parameter definitions are provided in Appendix A

Table 5

Specifications and cost of the chosen battery technology.

Parameter	Specification	Unit
Nominal voltage	6	V
Maximum capacity	376	Ah
Nominal capacity	2.26	kWh
Round-trip efficiency	80	%
Capital cost	174	€
Replacement cost	174	€
O&M cost	0	€/a
Lifetime	10	a
String size	8	-
Output (range)	0-5000	kWh

(Section A.1; Eq. (A.1) and (A.2)).

Additionally, all four systems have a panel azimuth of zero based on the HOMER optimizer, and the PV capacity is optimized. The PV has upper and lower bounds of 0 kW and 3000 kW, respectively. [Table 3](#) displays the specific details of the solar PV panels [39–41].

3.4.2. Wind turbine

The 100-kW XANT M 21 wind turbine (WT) was chosen for the investigation because it offers several advantages from an economic and technical performance standpoint [42]. Each wind turbine is assumed to have capital, replacement, and O&M expenses of 50,000 €/a, 30,000 €/a, and 2500 €/a, respectively. Based on the HOMER optimizer, the wind turbine's capacity is optimized. The upper and lower bounds of wind turbines are 20 kW and 0 kW, respectively. [Table 4](#) shows the wind turbine's parameterization adopted [43]. Detailed equations and parameter definitions are provided in [Appendix A](#) (Section A.2; Eq. (A.3), (A.4), and (A.5)).

3.4.3. Battery

The battery storage unit is intended to be used for this HRES due to the intermittent nature of the renewable energies wind and solar power during the days and months of the year. The HRES can be set up in such a way as to have a storage unit to assure the required constant voltage and reliability of the power supply [44].

The system was modeled in HOMER PRO using a storage unit that provides autonomous balancing between generation and load. HOMER's optimization engine determines the most cost-effective battery size by simulating different configurations across a defined capacity range (0–5000 kWh). In addition to cost considerations, the model accounts for technical limitations, including a defined battery lifetime of 10 years and a round-trip efficiency of 80 %. Although a minimum state of charge (SoC) threshold was not explicitly defined by the user, HOMER's internal logic maintains feasible SoC levels to prevent over-discharge, thereby implicitly capturing operational constraints.

Detailed equations and parameter definitions are provided in [Appendix A](#) (Section A.3; Eqs. (A.6), (A.7), (A.8), (A.9)), and [Table 5](#) displays the key technical and cost specifications of the selected battery technology.

3.4.4. Converter

The converter is used to transfer the energy flow between DC and AC [45]. According to the energy flow from a DC bus to an AC bus, the capacity required for an inverter is estimated (cf. [46]):

$$\eta_{inv} = \frac{P_o}{P_i}, \quad (5)$$

where P_i is the inverter's input power (kW) and P_o is its output power (kW).

The converter's initial, replacement, and O&M expenses are estimated to be 800, 750, and 8 €/kW/a, respectively. It is assumed that the converter has a 15-year lifespan and a 95 percent efficiency [21]. The converter's capacity is optimized by HOMER PRO. The converter's upper and lower bounds are 0 kW and 1000 kW, respectively. [Table 6](#) provides the exact specification details of the converter under consideration.

Table 6
Converter specifications.

Parameter	Specification	Unit
Capital cost	800	€
Replacement cost (after 15 years)	750	€
O&M cost	8	€/kW/a
Efficiency	95	%
Lifetime	15	a
Capacity (range)	0–1000	kW

4. Results

In this section, the results of the techno-economic analysis of hybrid renewable energy EVCSs in the four cities considered are reported. The configuration of three types of EVCS, which are PV, WT, and battery, are selected. [Table 7](#) shows the optimal configuration schemes for each city in the case of no capacity shortage.

[Table 7](#) shows, from an economic perspective, that the hybrid PV/WT/battery EVCS is the preferred option in Berlin, Hamburg, and Munich, but not for Cologne. In contrast, the economically most favorable configuration for EVCSs in Cologne is WT/battery. Across the cities, the most economical hybrid PV/WT/battery EVCS is in Cologne (0 kW PV, 4 WTs, 1192 batteries, and a 186 kW converter) with the minimum NPC, LCOE, and operating cost (OC), and initial capital cost (IC) of €882,891, 0.131 €/kWh, 25,171 €/a, and €557,496, while the PV/WT/battery (142 kW PV, 4 WTs, 2000 batteries, 196 kW converter) charging station in Munich is the least economical, with the maximum NPC, LCOE, OC, and IC at €1.23 M, 0.182 €/kWh, 26,331 €/a, and €890,937. In Cologne, although the WT/battery system has the lowest NPC, the hybrid PV/WT/battery system remains a competitive alternative with an NPC of €888,898. Across all four cities, the analysis demonstrates that renewables-based EVCSs offer clean and environmentally friendly solutions by reducing reliance on grid electricity and minimizing CO₂ emissions. In the following, a sensitivity analysis highlights the influence of storage capacity and load profiles on the economic performance of these systems.

The NPC and LCOE are two significant aspects in every project to make the critical decision. [Fig. 8](#) proves that based on the overall cost comparison in terms of NPC and LCOE, the design of hybrid charging stations in Cologne gives the best economic benefits. The monthly electric output from the best hybrid PV/WT/battery EVCSs in the four cities is shown in [Fig. 9](#). The highest amount of electricity generated from WTs in Berlin, Hamburg, Munich, and Cologne is in January; in addition, it can be concluded that Munich has a great economic potential for hybrid PV/WT systems. The maximum amount of electricity from PV arrays in Munich is produced in the month of May, and during summertime.

The total annual amount of electricity generated by the four hybrid PV/WT/battery EVCSs is shown in [Fig. 10](#). The maximum electricity production and wind power generation among the technological options considered are achieved by Hamburg's hybrid PV/WT/battery power generation system, with values of 1,264,836 kWh/a and 1,247,398 kWh/a, respectively. The maximum annual PV power generation that occurs in Munich is 169,467 kWh/a. Additionally, Munich's hybrid PV/WT/battery power generating system has the lowest electricity output, with a value of 1,041,323 kWh/a. Munich has a minimum WT power generation of 871,857 kWh/a, and Hamburg has a minimum PV power generation of 17,438 kWh/a.

4.1. Sensitivity analysis

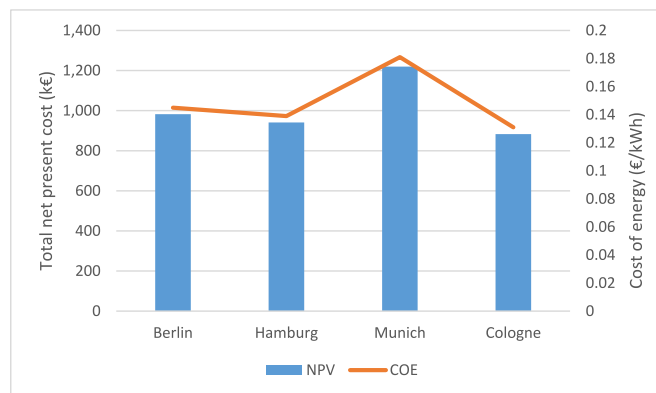
The main focus of the sensitivity analysis in this study is on the effects of demand load variation, capacity shortage, solar irradiation, and variations in wind speed on Munich's PV/WT/battery charging stations. [Table 8](#) displays the sensitivity variables' fluctuation range. It can be seen that the daily energy demand ranges from 935 kWh/d to 1935 kWh/d, the capacity shortage from 0 to 10 %, solar irradiation from 2.80 to 5.45 kWh/m²/d, and wind speed from 3.67 m/s to 7.52 m/s. [Fig. 11](#) shows the effect of the load change on PV/WT/battery EVCSs in Munich. It can be seen that the NPC of the charging station increases from €524,836 to €1,640,000 when the energy demand increases from 935 kWh/d to 1935 kWh/d. It can also be seen that the LCOE value of the charging station fluctuates around 0.181 €/kWh as demand increases. [Fig. 12](#) depicts how changes in load affect the excess electricity (EE) and unmet electric load (UEL) values of the PV/WT/battery EVCSs in Munich. As can be seen the EE value of the PV/WT/battery system

Table 7

Optimum configurations of renewable energy EVCSs in different locations.

Location	Configuration	PV (kW)	WT (#)	Battery (#)	Converter (kW)	NPC (€)	LCOE (€/kWh)	OC (€/a)	IC (€)
Berlin	PV/WT/battery	67.5	3	1904	186	982,628	0.145	20,380	719,159
	WT/battery	0	4	2056	198	993,101	0.147	21,350	717,099
	PV/battery	1328	0	6328	239	3.38 M	0.500	27,810	3.02 M
Hamburg	PV/WT/battery	16.7	3	2288	182	941,132	0.139	17,367	716,618
	WT/battery	0	2	3208	192	993,773	0.147	14,009	812,667
	PV/battery/	1602	0	5720	318	3.80 M	0.562	36,396	3.33 M
Munich	PV/WT/battery	102	5	1776	184	1.22 M	0.180	26,331	890,937
	WT/battery	0	6	2928	184	1.31 M	0.193	26,329	967,051
	PV/battery	1197	0	5448	356	3.18 M	0.470	27,940	2.56 M
Cologne	WT/battery	0	4	1192	186	882,891	0.131	25,171	557,496
	PV/WT/battery	50.1	3	1344	181	888,898	0.131	22,746	594,852
	PV/battery	1281	0	5464	359	3.32 M	0.490	31,847	2.90

Note: M stands for million.

**Fig. 8.** Comparison of total NPC and LCOE for the four cities in Germany studied.

increases from 154,854 kW/a to 1,047,426 kWh/a when the energy demand increases from 935 kWh/d to 1935 kWh/d. **Fig. 13** (a) displays the fluctuation of the NPC and LCOE values for the EVCS under various capacity shortages and charging load values. NPC values are represented via the graphical interface, while LCOE values are superimposed on the graphical interface. The NPC and LCOE values of the optimal system diminish from €883,348 to €527,338 and from 0.181 €/kWh to 0.131 €/kWh when the capacity shortage rises from 0 % to 10 %. The reduction in NPC and LCOE with increasing capacity shortage suggests that higher capacity shortages enhance system reliability and economic feasibility due to more effective management of energy resources. Therefore, it can be concluded that in the case of a capacity shortage, having the appropriate number of EVs can increase the charging station's efficiency and reliability (see **Fig. 13** (b)).

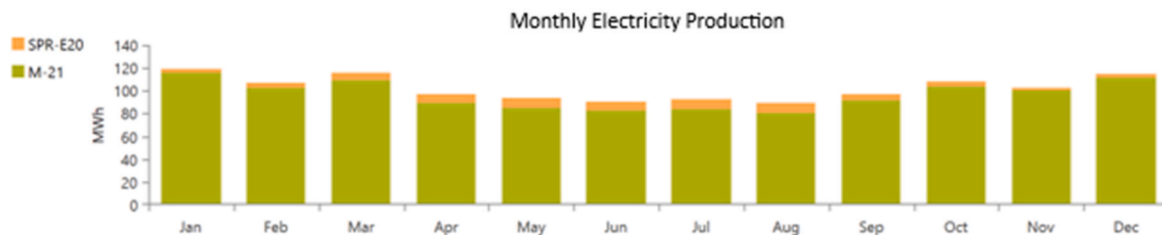
Fig. 13 (b) illustrates how the NPC and LCOE values of the EVCS change as a function of solar irradiation and wind speed values. It can be seen that the NPC and LCOE values of the optimal charging station decrease when solar irradiation rises from 2.07 kWh/m²/d to 5.45 kWh/m²/d at a particular wind speed. Moreover, the NPC and LCOE values of the optimal charging station decrease when the wind speed increases from 3.67 m/s to 7.52 m/s at a particular solar irradiation level. Furthermore, the effect of changes in both wind speed and solar irradiation on the NPV and LCOE is illustrated in **Fig. 14(a)** and (b), respectively. In other words, moderate increases in the values of solar irradiation and wind speed can significantly enhance the economic feasibility of the charging stations. It can also be deduced that improving the economic viability of EVCSs may be achieved by adopting PV tracking modes to boost the solar irradiation value, or by raising the hub height of the wind turbine in order to increase wind speed, or by using more economical battery technology.

4.2. Comparative analysis with grid connectivity

Although a large number of fast EVCS connections to the current grid may strain the network and have a detrimental influence on the security of power supply, it is important to consider whether it is economically feasible to choose a stand-alone or grid-connected EVCS. Therefore, in this section, the break-even distance is calculated for all four studied cities to determine how far from the network a stand-alone EVCS becomes more economically viable than a grid-connected system. **Table 9** shows the variables used in HOMER's grid-based EVCS simulation and optimization method. The grid cost data in this table are derived from real-world infrastructure cost assessments, as analyzed by Ahamer [47, 48]. **Table 10** presents the break-even distance at which both grid-connected and stand-alone optimal configuration EVCS NPCs are the same for each of the four selected cities in Germany. On the one hand, the hybrid renewable energy stand-alone system option is preferable from an economic perspective if the distance between the chosen EVCS location and the available grid is equal to or greater than the break-even distance. On the other hand, if it is lower, the grid-connected EVCS option is more desirable. **Fig. 15** shows the break-even distance graphically. If the grid is present at the EVCS location, the NPC is relatively low, but as the distance grows, it increases steadily. The lines denoting stand-alone NPC and grid-connected NPC intersect at a break-even distance. A separate EVCS solution would be more practical after this. The payback period for stand-alone and grid-connected selected cities are calculated and reflected in **Table 11**. The results show that the payback period for stand-alone systems in the four cities are lower than the payback period for grid-connected systems.

The calculated PI values for stand-alone hybrid renewable energy EVCSs in Berlin, Hamburg, Munich, and Cologne are 1.5, 1.2, 1.4, and 1.1, respectively, confirming the financial viability of these projects, as

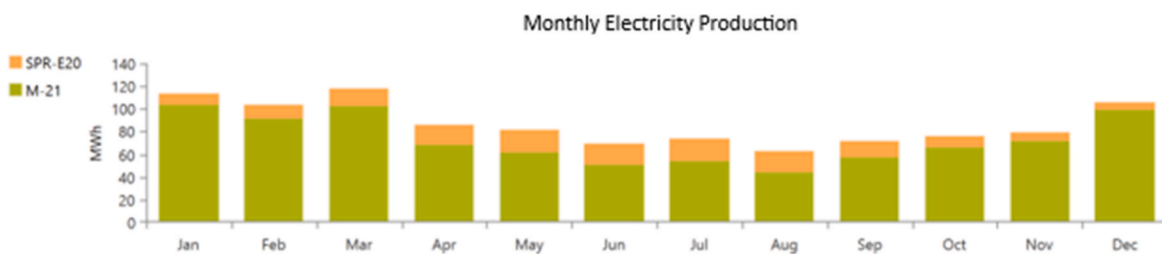
(a) Berlin



(b) Hamburg



(c) Munich



(d) Cologne



Fig. 9. The monthly electricity output of the PV/WT/battery charging stations in the four cities studied.

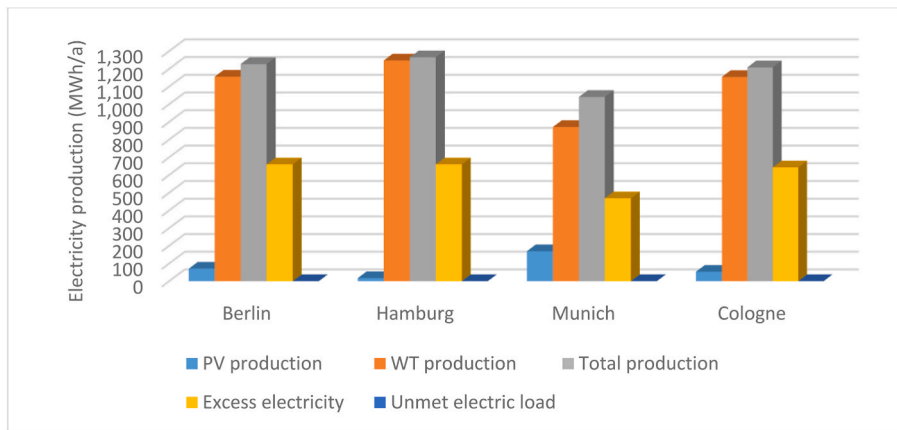


Fig. 10. Comparison of the total annual electricity production, excess and un-met electric load (UEL) of the four cities, various configurations of hybrid PV/WT/battery EVCSSs.

Table 8

The fluctuation range of sensitivity variables.

Energy demand (kWh/d)	Capacity shortage (%)	Solar irradiation (kWh/m ² /d)	Wind speed (m/s)
935	0	2.80	3.67
1035	1	2.07	3.98
1135	2	3.15	4.25
1235	3	3.36	4.56
1335	4	4.77	4.82
1435	5	4.33	5.15
1535	6	4.65	5.46
1635	7	4.87	5.77
1735	8	5.12	6.12
1835	9	5.34	7.23
1935	10	5.45	7.52

all values exceed the profitability threshold of 1.0. In contrast, the PI values for grid-connected EVCSSs in the same cities are 0.99, 0.87, 0.69, and 0.65, respectively, indicating lower profitability.

Finally, the IRR for stand-alone configurations in Berlin, Hamburg, Munich, and Cologne is 5.23 %, 4.62 %, 3.51 %, and 2.15, respectively. In comparison, the IRR calculated for grid-connected EVCS in these selected cities is lower at 2.16 %, 1.56 %, 1.14 %, and 0.87 %, respectively. Accordingly, the stand-alone hybrid renewable energy project is economically more attractive due to its higher IRR and greater potential returns.

5. Conclusions and future work

This study presented a comprehensive techno-economic assessment of stand-alone EVCSSs powered by hybrid PV, WT, and battery systems in four major German cities: Berlin, Munich, Hamburg, and Cologne. Using the HOMER PRO microgrid optimization software, various system configurations were modeled and simulated to identify cost-optimal setups that meet daily EV charging demand under region-specific renewable resource conditions. The results indicated that hybrid PV/WT/battery EVCSSs are the most cost-effective configurations for Berlin, Munich, and Hamburg, while a WT/battery system proved more suitable for Cologne due to better wind conditions and lower dependence on PV arrays. However, the hybrid PV/WT/battery system in Cologne remains a competitive economic alternative, particularly under scenarios of increased solar availability. Seasonal generation patterns revealed that wind power production in all four cities peaked in January, while PV arrays delivered maximum output in May, particularly in Munich, which demonstrates high potential for PV integration.

The analysis also demonstrated that increasing the daily energy demand from 935 kWh/d to 1935 kWh/d led to a significant rise in NPC of the charging station in Munich, although LCOE remained stable at around 0.181 €/kWh, indicating that higher loads impact investment requirements more than per-unit energy costs. Additionally, increased energy demand improved system utilization, as total annual electricity generation rose markedly. Allowing for capacity shortages of up to 10 %

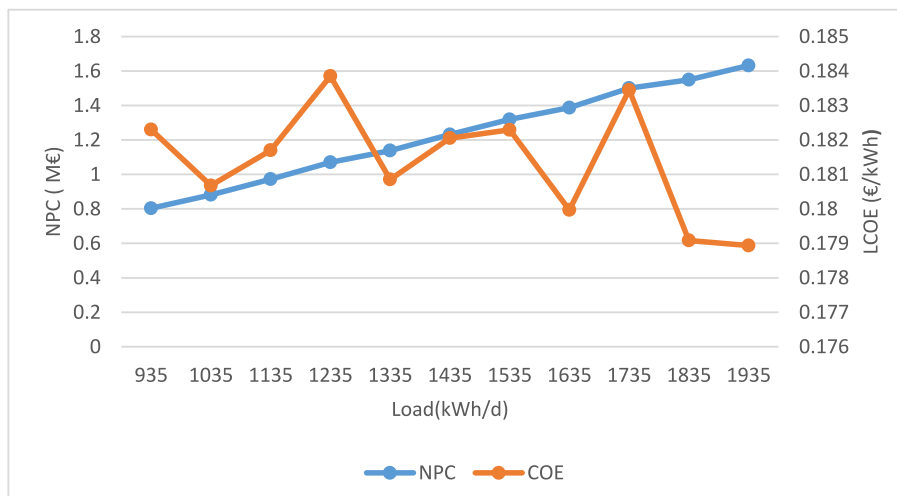


Fig. 11. The effects of energy demand variation on Munich's PV/WT/battery charging stations.

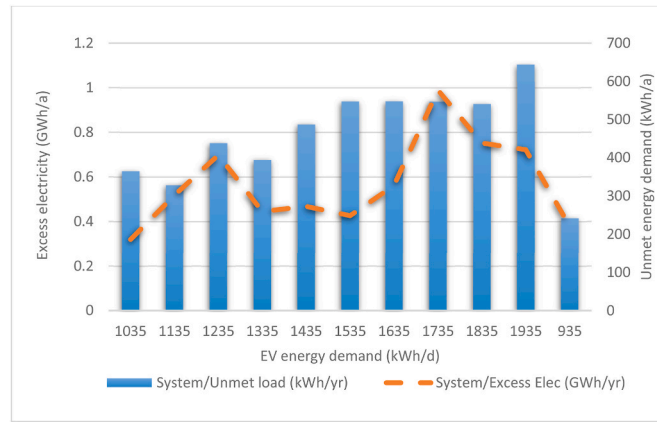


Fig. 12. The effects of energy demand change on excess electricity (EE) and un-met electric load (UEL) values of the PV/WT/battery EVCSs in Munich.

significantly improved both economic and operational performance, reducing NPC and LCOE by approximately 40 % and 28 %, respectively. This improvement is attributed to better resource management under constrained capacity conditions. Moreover, the sensitivity analysis confirmed that moderate improvements in solar irradiation (from 2.07

$\text{kWh/m}^2/\text{d}$ to 5.45 $\text{kWh/m}^2/\text{d}$) and wind speed (from 3.67 m/s to 7.52 m/s) further enhanced system economics. Practical design strategies—such as implementing PV tracking systems and increasing wind turbine hub heights—can increase resource availability but may incur additional capital and maintenance costs. However, these strategies may

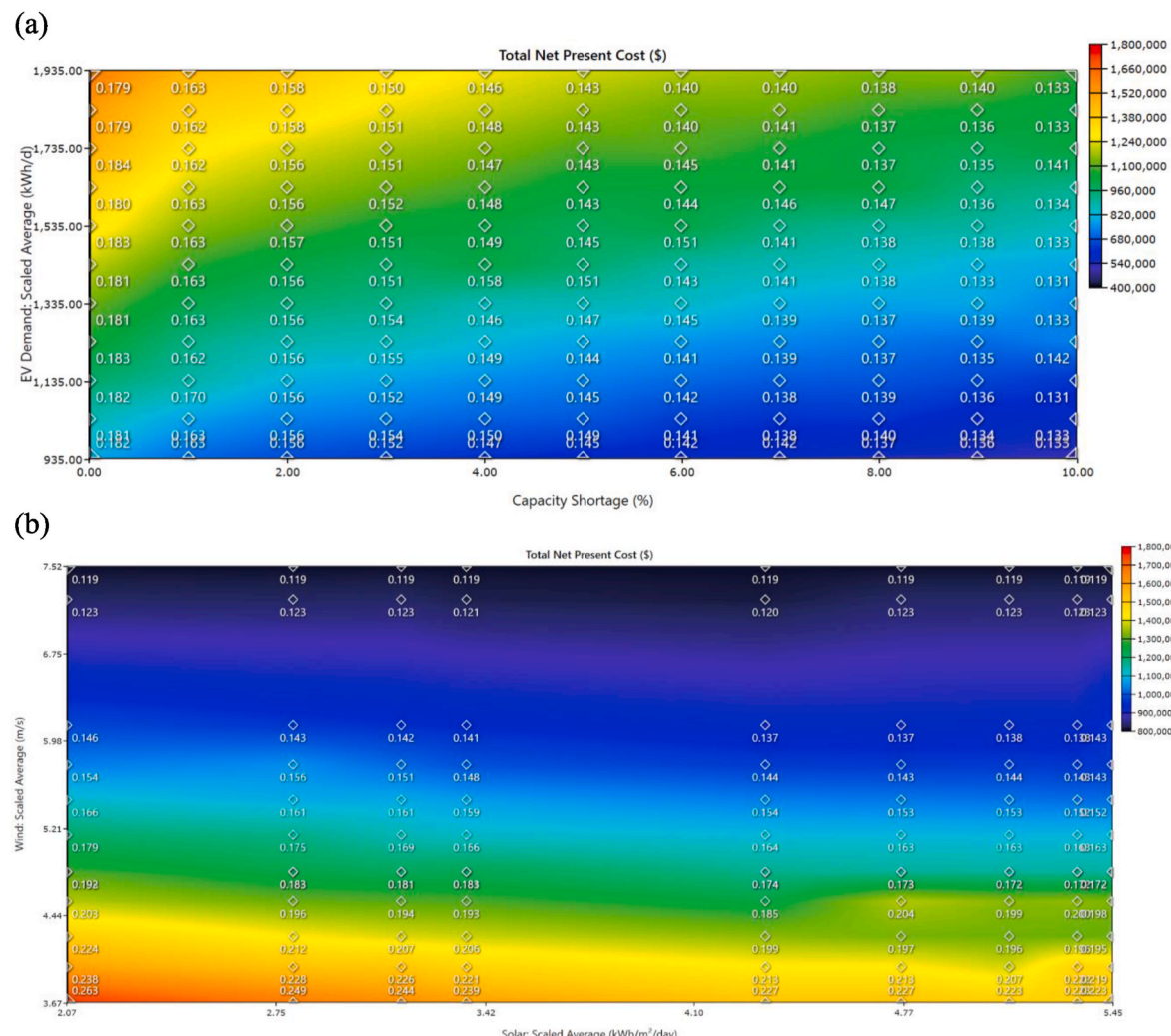


Fig. 13. Impact of two key variables on the charging station's NPC and LCOE in Munich.
 (a) Capacity shortage (x-axis) and EV demand (y-axis).
 (b) Solar irradiation (x-axis) and wind speed (y-axis).

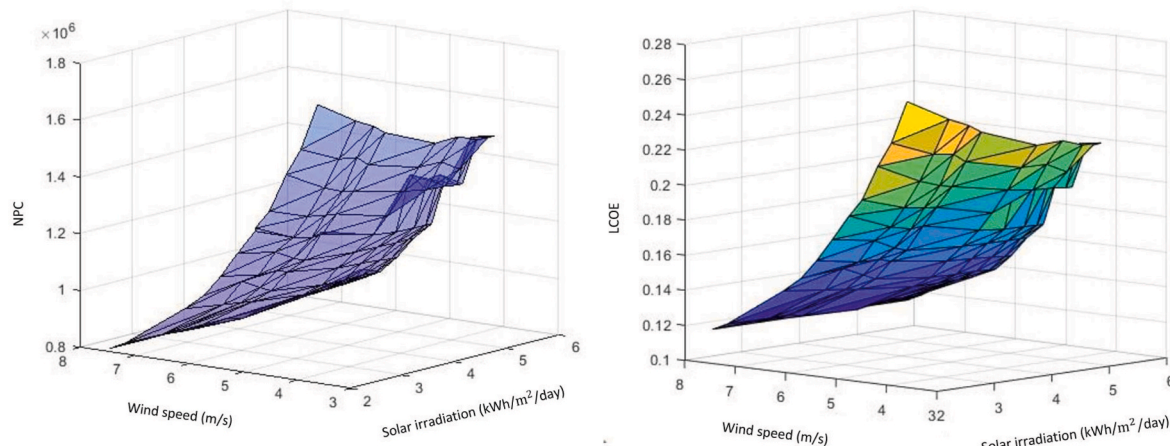


Fig. 14. (b) LCOE. The effects of changes in wind speed and solar irradiation in Munich.

Table 9
Costs related to the grid connection.

Description	Value	Unit
Grid tariff	0.08	€/kWh
Grid capital unit cost	1,500,000	€/km

also lead to higher maintenance and capital costs, which should be accounted for in long-term economic assessments. Furthermore, a break-even distance analysis showed that stand-alone systems become more economically viable than grid-connected options beyond certain thresholds, varying by city. These thresholds indicate the point at which the increasing cost of grid extension surpasses the relatively stable cost of decentralized systems. Among all cases, Berlin achieved the highest IRR at 5.23 %.

Future research should explore integrating additional renewable energy sources such as biomass or hydrogen to enhance the resilience and efficiency of stand-alone EV charging systems. In parallel, the use of advanced optimization techniques, including machine learning and scenario-based simulations, could enable more adaptive system planning under variable demand and resource conditions. Furthermore, refining EV load estimation through socio-demographic, geographic, and behavioral data would significantly improve the spatial accuracy of infrastructure planning, particularly in complex urban environments. Additionally, future work should focus on more detailed battery modeling, including temperature-dependent degradation, real-time state of charge (SoC) tracking, and adaptive control of depth of discharge (DoD). These enhancements would enable a more realistic evaluation of battery performance and lifecycle costs under diverse climatic and operational conditions.

The findings of this study offer practical guidance for the regional deployment of renewables-powered EV charging systems, reinforcing Germany's broader strategies for sustainable mobility and deep decarbonization.

Table 10
Optimal design break-even distance for the four selected cities in Germany.

Optimal configuration location	NPC (€)	LCOE (€)	Break-even distance (km)
Berlin	982,628	0.145	1.83
Hamburg	906,795	0.134	1.67
Munich	1,216,692	0.180	2.3
Cologne	897,412	0.132	1.65

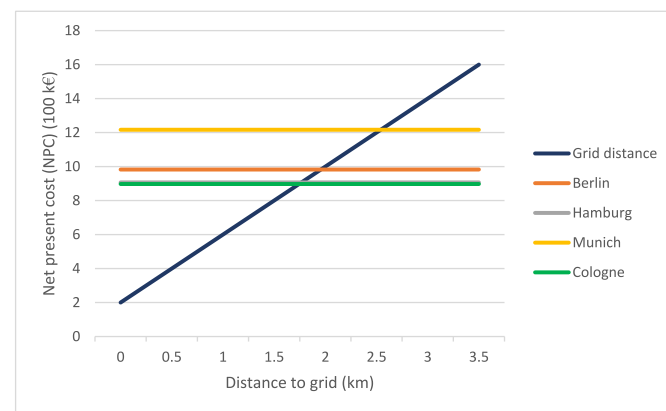


Fig. 15. Break-even distance for each of the four selected cities in Germany.

Table 11
Stand-alone and grid-connected EVCS payback times in the four selected cities in Germany.

City	Stand-alone payback period (a)	Grid-connected payback period (a)
Berlin	4	8
Hamburg	10	15
Munich	16	21
Cologne	19	23

CRediT authorship contribution statement

Rahil Dejkam: Conceptualization, Data curation, Formal analysis, Investigation, Methodology, Validation, Visualization, Writing – original draft. **Reinhard Madlener:** Conceptualization, Funding acquisition, Project administration, Resources, Supervision, Validation, Visualization, Writing – review & editing.

Declaration of competing interest

The authors declare that they have no known competing financial interests or personal relationships that could have appeared to influence the work reported in this paper.

Appendix A. Technical Modeling Equations and Parameters

A.1. PV module

It is assumed that the PV module has a lifetime of 25 years, with a typical annual degradation rate of approximately 0.5 % per year due to material wear and environmental factors. In HOMER, the photovoltaic derating factor represents the overall efficiency losses under real-world operating conditions compared to the ideal rated power of the PV module. This includes system inefficiencies such as inverter losses, temperature effects, dust accumulation, and wiring losses, rather than solely the deterioration of solar cells. In this study, a derating factor of 88 % is applied, meaning that only 88 % of the nominal PV capacity is available under normal operating conditions, considering these real-world losses. The degradation of PV cells over time is accounted for separately through an annual efficiency reduction, which is not included in the fixed derating factor [49].

The PV arrays in Berlin, Hamburg, Munich, and Cologne were installed at fixed slopes of 30 °, 35 °, 32 °, and 30.6 °, respectively, without tracking devices. Since this study does not incorporate local economic or spatial data, the use of tracking systems was not considered, as their feasibility strongly depends on these factors. While tracking systems can increase energy yield by 20–30 %, their higher installation and maintenance costs often outweigh the benefits, especially under Germany's moderate solar irradiance conditions [50,51].

According to data from the PV-GIS website, the optimal fixed slope angle for PV systems in Germany ranges between 35 ° and 40 °, as shown in Figure A.1(a). However, in this study, a 30.6 ° slope angle—originally applied in France by Saint-Drenan et al. [52]—was also considered for Germany due to land-use optimization strategies that prioritize higher module density. Figure A.1(b) presents the average slope angle value in the French study, assumed to be 30.6°. Reducing the slope angle below the optimal range allows for increased PV capacity per unit area, which can boost overall energy output, even if individual panel efficiency is slightly lower [53].

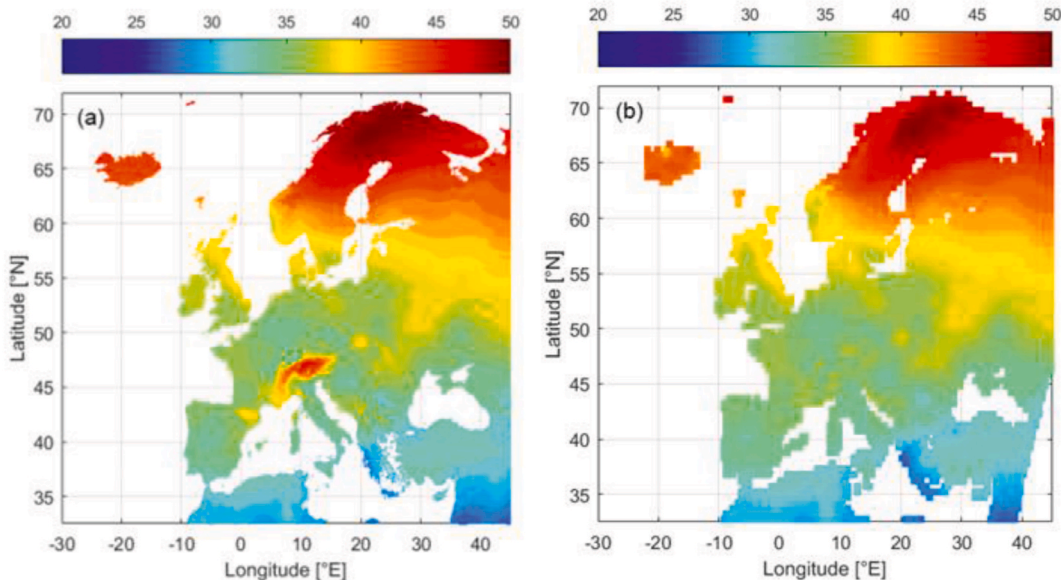


Fig. A.1. Optimal PV module slope angles (a) From the PV-GIS website [54]. (b) Applied in Europe including France in 2015 by Saint-Drenan et al. [52].

In the HOMER optimizer, the PV's output power is expressed as (see Ref. [50]):

$$P_{PV} = Y_{PV} \times f_{PV} \times \frac{I_T}{1000} \times [1 + \alpha(T_c - T_s)] \quad (A.1)$$

where I_T is the total solar irradiation incident on the PV panels, Y_{PV} is the nominal power of the PV panels, f_{PV} is the derating factor, α is the temperature coefficient, T_c is the cell temperature, and I_s is the cell temperature under Standard Test Conditions (STC). The cell temperature is estimated as follows [55]:

$$T_c(t) = T_a(t) + \left(\frac{NOCT - 20}{0.8} \right) \times \frac{I_T}{I_s} \quad (A.2)$$

where T_a is the time-dependent ambient temperature in degrees Celsius and NOCT is the nominal operating cell temperature.

A.2. Wind turbine

In practical applications, the exponential law model is typically used to calculate wind speed variation with height and terrain. The exponential law calculates wind speeds at various hub heights and anemometer heights. The following is a proxy formula for applying the exponential law to the calculations (see Refs. [56,57]):

$$\frac{v_{hub}}{v_{ane}} = \left(\frac{h_{hub}}{h_{ane}} \right)^a \quad (A.3)$$

where h_{ane} is the anemometer height of the wind turbine (m), h_{hub} is the hub height (m), v_{ane} is the wind speed at anemometer height of the WT (m/s), v_{hub} is the wind speed at hub height (m/s), and a is the power law exponent, which ranges from 0.05 to 0.5 depending on surface roughness and atmospheric stability. In this research, the selected locations' values were taken to be 0.14.

The energy production characteristics of the WT at various hub height wind speeds can be seen in the power curve of the WT. Figure A.2 depicts the output power curve of the XANT M 21 WT [43]. The output power of the WT ($P_{ws}(v)$), which is approximately represented by the power curve under the determined wind speed (v), is shown in Eq. (A.4). The power curve depicts the performance of the WT at standard temperatures and pressures (STP) (cf. [58]).

$$P_{ws}(v) = \begin{cases} 0, v < v_{in} \text{ or } v > v_{out} \\ \frac{P_r \cdot (v - v_{in})}{(v_r - v_{in})}, v_{in} \leq v \leq v_r \\ P_r, v_r \leq v \leq v_{out} \end{cases} \quad (\text{A.4})$$

where P_r is the rated power of the wind turbine (kW), v_{in} is the cut-in wind speed of the WT (m/s), v_r is the rated wind speed of the WT (m/s), and v_{out} is the cut-out wind speed of the WT (m/s).

The following Eq. (A.5) enables an approximation of the output power of a WT ($P_w(v)$) under real-world circumstances (see Ref. [58]):

$$P_w(v) = P_{ws}(v) \cdot \frac{\rho}{1.225} \quad (\text{A.5})$$

where ρ is the actual air density (kg/m³).

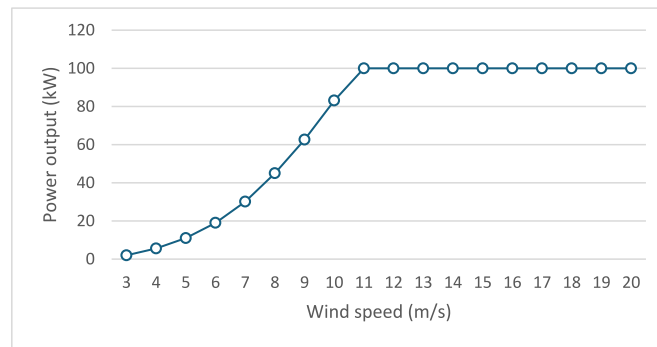


Fig. A.2 Power curve of the XANT M-21 WT.

A.3. Battery

The voltage and nominal capacity are the variables that impact battery efficiency. Equations (A.6) and (A.7) can be used to derive battery efficiency and voltage [59], whereas battery storage is essential in maximizing the renewable energy output, determined by Eq. (A.8) (see Ref. [60]):

$$\eta_{batt} = 1 - \left(\frac{I_{nom} \times R_{int} \times I_{nom}}{V_{nom} \times I_{nom}} \right) \quad (\text{A.6})$$

$$V_{batt} = E_0 - (R_{int} \times I_{batt}) \quad (\text{A.7})$$

$$P_{max,b} = \frac{N_{batt} \times V_{batt} \times I_{max}}{1000} \quad (\text{A.8})$$

where I_{batt} is the battery current, R_{int} is the internal resistance, and E_0 is the no-load voltage level. The nominal voltage is V_{nom} , and the nominal current is I_{nom} . I_{max} denotes the battery's maximum current, and N_{batt} stands for the number of batteries. The formula for calculating battery capacity (kW) is as follows (see Ref. [61]):

$$C_B = \frac{E_L \times AD}{DOD \times \eta_{in} \times \eta_{batt}} \quad (\text{A.9})$$

where E_L stands for overall energy demand, AD for autonomous days, and DOD for discharge depth. Inverter and battery efficiency are represented by η_{in} and η_{batt} , respectively. A Trojan SSIG deep-cycle lead-acid battery with 6 V, 376 Ah has been selected for this simulation due to its cost-effectiveness, reliability, and well-documented performance characteristics. Despite the emergence of lithium-ion alternatives, lead-acid batteries remain widely used in stand-alone and renewable energy applications due to their lower upfront costs, deep-cycle capability, and maintenance-free operation, making them suitable for frequent charge-discharge cycles [62]. Its efficiency is considered to be 80 %, and its expected lifespan 13 years [63]. The cost estimates for battery investment, replacement, and maintenance are 174 €/kW, 174 €/kW, and 0 €/kW, respectively [64–66].

Data availability

Data will be made available on request.

References

- [1] Eltoumi FM, Becherif M, Djerdir A, Ramadan Haitham S. The key issues of electric vehicle charging via hybrid power sources: techno-economic viability, analysis, and recommendations. *Renew Sustain Energy Rev* 2021;138:110534. <https://doi.org/10.1016/j.rser.2020.110534>.
- [2] Tang C, Tukker A, Sprecher B, Mogollón JM. Assessing the European electric-mobility transition: emissions from electric vehicle manufacturing and use in relation to the EU greenhouse gas emission targets. *Environ Sci Technol* 2023;57:44–52. <https://doi.org/10.1021/acs.est.2c06304>.
- [3] Liu X, Sun X, Zheng H, Huang D. Do policy incentives drive electric vehicle adoption? Evidence from China. *Transp Res Part Policy Pract* 2021;150:49–62. <https://doi.org/10.1016/j.trap.2021.05.013>.
- [4] Tan Z, Tan Q, Rong M. Analysis on the financing status of PV industry in China and the ways of improvement. *Renew Sustain Energy Rev* 2018;93:409–20. <https://doi.org/10.1016/j.rser.2018.05.036>.
- [5] Yu H, Dai H, Tian G, Wu B, Xie Y, Zhu Y, et al. Key technology and application analysis of quick coding for recovery of retired energy vehicle battery. *Renew Sustain Energy Rev* 2021;135:110129. <https://doi.org/10.1016/j.rser.2020.110129>.
- [6] Liu W, Zeng L, Wang Q. Psychological distance toward air pollution and purchase intention for new energy vehicles: an investigation in China. *Front Psychol* 2021;12:569115. <https://doi.org/10.3389/fpsyg.2021.569115>.
- [7] Ma H, Balthasar F, Tait N, Riera-Palou X, Harrison A. A new comparison between the life cycle greenhouse gas emissions of battery electric vehicles and internal combustion vehicles. *Energy Policy* 2012;44:160–73. <https://doi.org/10.1016/j.enpol.2012.01.034>.
- [8] Zhou C, Qi S, Zhang J, Tang S. Potential Co-benefit effect analysis of orderly charging and discharging of electric vehicles in China. *Energy* 2021;226:120352. <https://doi.org/10.1016/j.energy.2021.120352>.
- [9] Burkert A, Fechtner H, Schmuelling B. Interdisciplinary analysis of social acceptance regarding electric vehicles with a focus on charging infrastructure and driving range in Germany. *World Electr Veh J* 2021;12:25. <https://doi.org/10.3390/wevj2010025>.
- [10] Schetinger AM, Dias DHN, Borba BSMC, Pimentel da Silva GD. Techno-economic feasibility study on electric vehicle and renewable energy integration: a case study. *Energy Storage* 2020;2. <https://doi.org/10.1002/est2.197>.
- [11] Drücke J, Borsche M, James P, Kaspar F, Pfeifroth U, Ahrens B, et al. Climatological analysis of solar and wind energy in Germany using the Grosswetterlagen classification. *Renew Energy* 2021;164:1254–66. <https://doi.org/10.1016/j.renene.2020.10.102>.
- [12] Al-Quraan A, Al-Mhairat B. Economic predictive control-based sizing and energy management for grid-connected hybrid renewable energy systems. *Energy* 2024;302:131795. <https://doi.org/10.1016/j.energy.2024.131795>.
- [13] Al-Quraan A, Athamnah I. Economic predictive tri-level control for efficiency maximization of stand-alone hybrid renewable energy system. *J Power Sources* 2024;596:234098. <https://doi.org/10.1016/j.jpowsour.2024.234098>.
- [14] Al-Quraan A, Athamnah I. Economic tri-level control-based sizing and energy management optimization for efficiency maximization of stand-alone HRES. *Energy Convers Manag* 2024;302:118140. <https://doi.org/10.1016/j.enconman.2024.118140>.
- [15] Al-Quraan A, Athamnah I, Malkawi AMA. Efficiency maximization of stand-alone HRES based on tri-level economic predictive technique. *Sustainability* 2024;16:10762. <https://doi.org/10.3390/su162310762>.
- [16] Al-Quraan A, Al-Mhairat B, Malkawi AMA, Radaideh A, Al-Masri HMK. Optimal prediction of wind energy resources based on WOA—A case study in Jordan. *Sustainability* 2023;15:3927. <https://doi.org/10.3390/su15053927>.
- [17] Al-Quraan A, Al-Mharat B, Koran A, Radaideh AG. Performance improvement of a standalone hybrid renewable energy system using a bi-level predictive optimization technique. *Sustainability* 2025;17:725. <https://doi.org/10.3390/su17020725>.
- [18] Al-Quraan A, Al-Mhairat B. Sizing and energy management of standalone hybrid renewable energy systems based on economic predictive control. *Energy Convers Manag* 2024;300:117948. <https://doi.org/10.1016/j.enconman.2023.117948>.
- [19] Al-Quraan A, Al-Mhairat B. Sizing and energy management of grid-connected hybrid renewable energy systems based on techno-economic predictive technique. *Renew Energy* 2024;228:120639. <https://doi.org/10.1016/j.renene.2024.120639>.
- [20] Al Wahedi A, Bicer Y. Techno-economic optimization of novel stand-alone renewables-based electric vehicle charging stations in Qatar. *Energy* 2022;243:123008. <https://doi.org/10.1016/j.energy.2021.123008>.
- [21] Li C, Shan Y, Zhang L, Zhang L, Fu R. Techno-economic evaluation of electric vehicle charging stations based on hybrid renewable energy in China. *Energy Strategy Rev* 2022;41:100850. <https://doi.org/10.1016/j.esr.2022.100850>.
- [22] Ekren O, Hakan Canbaz C, Güvel CB. Sizing of a solar-wind hybrid electric vehicle charging station by using HOMER software. *J Clean Prod* 2021;279:123615. <https://doi.org/10.1016/j.jclepro.2020.123615>.
- [23] Karmaker AK, Ahmed MdR, Hossain MdA, Sikder MdM. Feasibility assessment & design of hybrid renewable energy based electric vehicle charging station in Bangladesh. *Sustain Cities Soc* 2018;39:189–202. <https://doi.org/10.1016/j.scs.2018.02.035>.
- [24] Karmaker AK, Hossain MdA, Manoj Kumar N, Jagadeesan V, Jayakumar A, Ray B. Analysis of using biogas resources for electric vehicle charging in Bangladesh: a techno-economic-environmental perspective. *Sustainability* 2020;12:2579. <https://doi.org/10.3390/su12072579>.
- [25] Grande LSA, Yahyaoui I, Gómez SA. Energetic, economic and environmental viability of off-grid PV-BESS for charging electric vehicles: case study of Spain. *Sustain Cities Soc* 2018;37:519–29. <https://doi.org/10.1016/j.scs.2017.12.009>.
- [26] Chandra Mouli GR, Bauer P, Zeman M. System design for a solar powered electric vehicle charging station for workplaces. *Appl Energy* 2016;168:434–43. <https://doi.org/10.1016/j.apenergy.2016.01.110>.
- [27] Vermaak HJ, Kusakana K. Design of a photovoltaic–wind charging station for small electric Tuk-tuk in D.R.Congo. *Renew Energy* 2014;67:40–5. <https://doi.org/10.1016/j.renene.2013.11.019>.
- [28] Alghoul MA, Hammadi FY, Amin N, Asim N. The role of existing infrastructure of fuel stations in deploying solar charging systems, electric vehicles and solar energy: a preliminary analysis. *Technol Forecast Soc Change* 2018;137:317–26. <https://doi.org/10.1016/j.techfore.2018.06.040>.
- [29] Dong X-J, Shen J-N, Ma Z-F, He Y-J. Stochastic optimization of integrated electric vehicle charging stations under photovoltaic uncertainty and battery power constraints. *Energy* 2025;314:134163. <https://doi.org/10.1016/j.energy.2024.134163>.
- [30] Tabassum S, Vijay Babu AR, Dheer DK. Adaptive energy management strategy for sustainable xEV charging stations in hybrid microgrid architecture. *Sci Technol Energy Transit* 2025;80:22. <https://doi.org/10.2516/stet/2025002>.
- [31] Esfilar R, Bagheri M, Golestanib A. Technoeconomic feasibility review of hybrid waste to energy system in the campus: a case study for the University of Victoria. *Renew Sustain Energy Rev* 2021;146:111190. <https://doi.org/10.1016/j.rser.2021.111190>.
- [32] Abo-Elyousr FK, Elnozahy A. Bi-objective economic feasibility of hybrid micro-grid systems with multiple fuel options for islanded areas in Egypt. *Renew Energy* 2018;128:37–56. <https://doi.org/10.1016/j.renene.2018.05.066>.
- [33] Burger B. Electricity production from solar and wind in Germany in 2014. *Fraunhofer ISE*, Freiburg/B.; 2014.
- [34] Statista Electric passenger cars in German cities 2024. <https://www.statista.com/statistics/2125/german-cities-electric-vehicle/>.
- [35] Google Maps. Google maps n.d. <https://www.google.de/maps/place/Germany/>. [accessed June 9, 2025].
- [36] Bansal S, Zong Y, You S, Mihet-Popă L, Xiao J. Technical and economic analysis of one-stop charging stations for battery and fuel cell EV with renewable energy sources. *Energies* 2020;13:2855. <https://doi.org/10.3390/en13112855>.
- [37] NASA POWER. Prediction of worldwide energy resources n.d. <https://power.larc.nasa.gov/>. [accessed July 14, 2025].
- [38] Clairand J-M, Alvarez-Bel C, Rodríguez-García J, Escrivá-Escrivá G. Impact of electric vehicle charging strategy on the long-term planning of an isolated microgrid. *Renewables* 2020;13:3455. <https://doi.org/10.3390/en13133455>.
- [39] Bandyopadhyay S, Mouli GRC, Qin Z, Elizondo LR, Bauer P. Techno-economic model based optimal sizing of PV-Battery systems for microgrids. *IEEE Trans Sustain Energy* 2020;11:1657–68. <https://doi.org/10.1109/TSTE.2019.2936129>.
- [40] Chowdhury T, Chowdhury H, Hasan S, Rahman MS, Bhuiya MMK, Chowdhury P. Design of a stand-alone energy hybrid system for a makeshift health care center: a case study. *J Build Eng* 2021;40:102346. <https://doi.org/10.1016/j.jobe.2021.102346>.
- [41] Das BK, Tushar MSHK, Zaman F. Techno-economic feasibility and size optimisation of an off-grid hybrid system for supplying electricity and thermal loads. *Energy* 2021;215:119141. <https://doi.org/10.1016/j.energy.2020.119141>.
- [42] Ribbing S, Xydis G. Renewable energy at home: a look into purchasing a wind turbine for home use—the cost of blindly relying on one tool in decision making. *Cleanroom Technol* 2021;3:299–310. <https://doi.org/10.3390/cleantech3020017>.
- [43] Nasab NM, Kilby J, Bakhtiyarifard L. Case study of a hybrid wind and tidal turbines system with a microgrid for power supply to a remote off-grid community in New Zealand. *Energies* 2021;14. <https://doi.org/10.3390/en14123636>.
- [44] Zakeri B, Syri S. Electrical energy storage systems: a comparative life cycle cost analysis. *Renew Sustain Energy Rev* 2015;42:569–96. <https://doi.org/10.1016/j.rser.2014.10.011>.
- [45] Lau KY, Tan CW, Yatim AHM. Photovoltaic systems for Malaysian islands: effects of interest rates, diesel prices and load sizes. *Energy* 2015;83:204–16. <https://doi.org/10.1016/j.energy.2015.02.015>.
- [46] Das BK, Hasan M, Rashid F. Optimal sizing of a grid-independent PV/diesel/pump-hydro hybrid system: a case study in Bangladesh. *Sustain Energy Technol Assessments* 2021;44:100997. <https://doi.org/10.1016/j.seta.2021.100997>.
- [47] Ahamer G. Cost of energy infrastructure in Europe and Austria: electricity, gas, oil, and heat. *Int J Glob Environ Issues* 2021;20:167. <https://doi.org/10.1504/IJGENVI.2021.121008>.
- [48] Clean Energy Wire. What German households pay for electricity, Clean Energy Wire (CLEW) - Journalism for the Energy Transition. <https://www.cleanenergywire.org/factsheets/what-german-households-pay-electricity>. [Accessed 25 February 2025].
- [49] PV derating factor n.d. https://www.homerenergy.com/products/pro/docs/latest/pv_derating_factor.html [accessed July 14, 2025].
- [50] Elahi Gol A, Ščasný M. Techno-economic analysis of fixed versus sun-tracking solar panels. *Int J Renew Energy Dev* 2023;12:615–26. <https://doi.org/10.14710/ijred.2023.50165>.
- [51] Bahrami A, Okoye CO. The performance and ranking pattern of PV systems incorporated with solar trackers in the northern hemisphere. *Renew Sustain Energy Rev* 2018;97:138–51. <https://doi.org/10.1016/j.rser.2018.08.035>.

[52] Saint-Drenan YM, Bofinger S, Fritz R, Vogt S, Good GH, Dobschinski J. An empirical approach to parameterizing photovoltaic plants for power forecasting and simulation. *Sol Energy* 2015;120:479–93. <https://doi.org/10.1016/j.solener.2015.07.024>.

[53] Saint-Drenan Y-M, Wald L, Ranchin T, Dubus L, Troccoli A. An approach for the estimation of the aggregated photovoltaic power generated in several European countries from meteorological data. *Adv Sci Res* 2018;15:51–62. <https://doi.org/10.5194/asr-15-51-2018>.

[54] European Commission. Photovoltaic geographical information system (PVGIS), Joint Research Centre. 2025, https://joint-research-centre.ec.europa.eu/photovoltaic-geographical-information-system-pvgis_en. [Accessed 24 February 2025].

[55] Kaabeche A, Bakelli Y. Renewable hybrid system size optimization considering various electrochemical energy storage technologies. *Energy Convers Manag* 2019; 193:162–75. <https://doi.org/10.1016/j.enconman.2019.04.064>.

[56] Artigao E, Viguera-Rodríguez A, Honrubia-Escribano A, Martín-Martínez S, Gómez-Lázaro E. Wind resource and wind power generation assessment for education in engineering. *Sustainability* 2021;13:2444. <https://doi.org/10.3390/su13052444>.

[57] Ohunakin OS, Adaramola MS, Oyewola OM. Wind energy evaluation for electricity generation using WECS in seven selected locations in Nigeria. *Appl Energy* 2011; 88:3197–206. <https://doi.org/10.1016/j.apenergy.2011.03.022>.

[58] Li C. Technical and economic potential evaluation of an off-grid hybrid wind-fuel cell-battery energy system in Xining, China. *Int J Green Energy* 2021;18:258–70. <https://doi.org/10.1080/15435075.2020.1854267>.

[59] Singh A, Baredar P, Gupta B. Techno-economic feasibility analysis of hydrogen fuel cell and solar photovoltaic hybrid renewable energy system for academic research building. *Energy Convers Manag* 2017;145:398–414. <https://doi.org/10.1016/j.enconman.2017.05.014>.

[60] How HOMER calculates the maximum battery charge power n.d. https://www.homerenergy.com/products/pro/docs/3.13/how_homer_calculates_the_maximum_battery_charge_power.html. [Accessed 14 July 2025].

[61] Borhanazad H, Mekhilef S, Gounder Ganapathy V, Modiri-Delshad M, Mirtaheri A. Optimization of micro-grid system using MOPSO. *Renew Energy* 2014;71:295–306. <https://doi.org/10.1016/j.renene.2014.05.006>.

[62] Diouf B, Pode R. Potential of lithium-ion batteries in renewable energy. *Renew Energy* 2015;76:375–80. <https://doi.org/10.1016/j.renene.2014.11.058>.

[63] Modified kinetic battery model n.d https://www.homerenergy.com/products/pro/docs/3.13/modified_kinetic_battery_model.html. [accessed July 14, 2025].

[64] Rezli H, Abdelkareem MA, Ghenai C. Performance evaluation and optimal design of stand-alone solar PV-battery system for irrigation in isolated regions: a case study in Al Minya (Egypt). *Sustain Energy Technol Assessments* 2019;36:100556. <https://doi.org/10.1016/j.seta.2019.100556>.

[65] Das BK, Hoque N, Mandal S, Pal TK, Raihan MA. A techno-economic feasibility of a stand-alone hybrid power generation for remote area application in Bangladesh. *Energy* 2017;134:775–88. <https://doi.org/10.1016/j.energy.2017.06.024>.

[66] Bhattacharyya SC. Mini-grid based electrification in Bangladesh: technical configuration and business analysis. *Renew Energy* 2015;75:745–61. <https://doi.org/10.1016/j.renene.2014.10.034>.